

Study on Interpretation Method of Multistage Fracture Tracer Flowback Curve in Tight Oil Reservoirs

Dianfa Du,* Fanghui Hao,* Yuan Li, Di Li, and Yujie Tang



Cite This: *ACS Omega* 2024, 9, 11628–11636



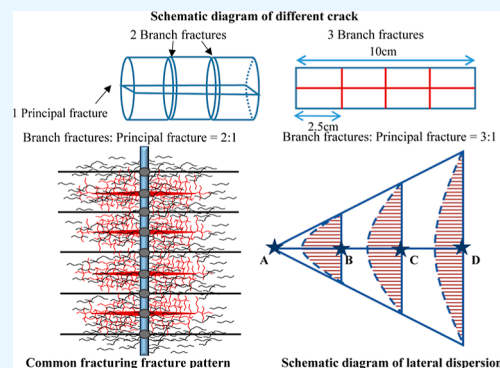
Read Online

ACCESS |

Metrics & More

Article Recommendations

ABSTRACT: Multistage fracturing is widely used in the development of tight oil reservoirs, and the fine description of postfracturing fracture networks is a challenge in tight oil reservoir development. Based on the formation mechanism of dual-wing fractures and the principles of tracer flowback, a mathematical model for tracer concentration in dual-wing fractures is established by considering the convective diffusion of the tracer within the fractures. An interpretation method for tracer flowback curves, utilizing a combination of Gaussian fitting and theoretical equation inversion, is developed to provide a detailed description of fracture parameters such as fracture half-length, fracture width, and fracture conductivity in the postfracturing fracture network. This method can be rapidly applied in field practices. Application examples demonstrate that the relative errors between the calculated cumulative oil and water production using this method and the actual data are less than 5%, validating the accuracy and applicability of the established mathematical model for tracer flowback and the interpretation method for tracer concentration curves in addressing practical problems.



1. INTRODUCTION

In recent years, tight oil reservoirs have become a focal point of global unconventional oil and gas exploration and development.^{1,2} Due to their characteristics such as significant reservoir thickness, low porosity and permeability, poor connectivity, and high water saturation, multistage fracturing technology has emerged as a key technique for reservoir stimulation in tight oil formations.^{3–5} With the widespread application of multistage fracturing technology in the development of tight reservoirs, accurately characterizing postfracturing fracture networks has become a challenging task in tight reservoir development. This characterization plays a crucial role in evaluating the effectiveness of fracturing and predicting production dynamics with a high level of accuracy.^{6,7} Currently, the commonly used methods for describing postfracturing fracture networks include microseismic event monitoring, production analysis, and fracturing fluid flowback analysis.^{8–11} During mining field operations, the injection and flowback technique of tracers is frequently employed.¹² Due to the infiltration of tracers in different fracture systems after fracturing, the resulting tracer flowback curves can vary. Therefore, analyzing tracer flowback curves allows for the determination of postfracturing fracture morphology and the acquisition of relevant fracture parameters.^{13–16} This method can also be utilized to evaluate different fracturing parameters and guide reservoir assessment, geological design (design of an oil field development plan), fracturing design, and workflow design.^{17,18} The tracer flowback curve is a tool used to study the flow pathways of fluids in underground

reservoirs. When tracers are injected into the reservoir, they move along with the fluid flow. By monitoring the arrival time and concentration of the tracers, tracer flowback curves can be plotted. These curves provide valuable information about the flow pathways of fluids in underground reservoirs and the microstructure of the reservoir.

The development of quantitative and qualitative analysis of tracer recovery, as well as the prediction of peak concentration and production time of tracer output curves, has laid the foundation for quantitative interpretation of tracers in oilfield applications. These advancements have significantly contributed to the substantial development of tracer technology in the oilfield industry.¹⁹ The derivation of the three-dimensional flow equation for tracer movement in fractures, considering the diffusion effect of the solution and the adsorption effect of the tracer, has achieved excellent results in field applications. This consideration of solution diffusion and tracer adsorption has enhanced the accuracy and effectiveness of tracer flow analysis in fractures.²⁰ By utilizing a neutron source and a gamma detector, it is possible to identify fracture proppants and determine

Received: November 8, 2023

Revised: February 12, 2024

Accepted: February 20, 2024

Published: February 29, 2024



fracture parameters by comparing the gamma-ray intensity emitted from activated materials in the proppants before and after fracturing. This technique allows for the identification of proppants used to support the fractures and the determination of fracture parameters.²¹ For non-Newtonian hydraulic fluids, once the fracture parameters governing their flow behavior are determined, the characteristics of underground fractures can be described through the interpretation of tracer flowback profiles using single-well tracer flowback analysis.²² Another method involves mixing tracer materials containing high thermal neutron capture cross-section elements with proppants and utilizing well logging techniques. By comparing the variations in the macroscopic neutron capture cross-section of the formation before and after fracturing, the position of proppants, fracture height, and other parameters related to the characteristics of the filled fractures can be determined.²³ The application of radioactive tracer technology in monitoring the fracturing process, along with the use of well logging techniques to reflect the changes in gamma-ray count rate of the tracer sand, enables the determination of fracture morphology parameters and further evaluation of the fracturing effectiveness.²⁴ To obtain fracture height parameters, the tracer diagnostic testing method can be employed. By detecting the distribution of tagged proppants around the wellbore, it is possible to interpret the near-wellbore fracture height, as well as the specific equivalent fracture widths for each layer. This information can be used to further evaluate the effectiveness of the fracturing operation.²⁵ To further characterize the flow state of the fracturing fluid, RTDA (residence time distribution analysis) has been combined with downhole tracers to determine the transition time from the fracture to the surface for each tracer section.²⁶ To provide a more comprehensive characterization of the flow behavior of fracturing fluids, the combination of residence time distribution analysis (RTDA) and downhole tracers can be utilized. This approach allows for the determination of the transit time from the fracture to the surface for each tracer segment, providing insights into the flow dynamics of the fracturing fluid.²⁷ In the context of multiphase flows, numerical simulation methods can be used to model the migration of tracers and radionuclides through heterogeneous fractured rocks in nonisothermal multiphase systems.²⁸ Semianalytical methods based on flow lines can also be utilized to simulate tracer movement through heterogeneous permeable media.²⁹ However, these methods are computationally complex and cannot be quickly applied to mining practice.

Based on the above, current research primarily focuses on tracer curve interpretation for conventional oil and gas reservoirs, while studies on unconventional reservoirs are limited. The use of tracer flowback techniques in these cases generally allows for qualitative analysis of fracture morphology but does not accurately describe postfracture parameters. As a result, precise characterization of postfracture fractures remains a challenging aspect of tight oil reservoir development in practical mining operations.

This study considers factors such as the tortuosity of fractures and establishes a mathematical model for tracer breakthrough concentration in dual-wing fractures. A tracer flowback curve interpretation method is developed using the “Gaussian fitting + theoretical equation inversion” approach, which accurately calculates parameters such as fracture half-length and fracture conductivity, enabling a quantitative description of postfracturing fractures in tight oil reservoirs. By employing the mathematical model and using the Gaussian fitting and

theoretical equation inversion method, the tracer flowback curves can be effectively interpreted, providing important information about the morphology of dual-wing fractures and tracer diffusion. The reliability and feasibility of this method are validated through experimental data and practical case studies.

2. DUAL-WING FRACTURE TRACER FLOWBACK PRINCIPLE

2.1. Mechanism of Dual-Wing Fracture Formation. The formation of dual-wing fractures requires specific conditions, namely when the brittle mineral content in tight reservoir rocks is less than 40%, the brittle index is less than 40%, the horizontal stress difference coefficient is greater than 0.25, and natural fractures are not developed in the tight reservoir. Under these circumstances, dual-wing fractures can be formed using conventional fracturing methods.

Traditional fracturing techniques rely on tuning properties such as proppant roundness and strength to enhance the permeability of the proppant pack, but they do not address the longitudinal permeability of the fracture itself. As a result, the width of the formed dual-wing fractures is generally small, typically ranging from 1 to 3 mm.

The improved technique involves the application of pulse fracturing with the injection of fibers as special proppants into the formation. This process establishes larger noncontinuous channels, significantly enhancing the fracture conductivity of dual-wing fractures. When describing the pore structure of dual-wing fractures under this scenario, their permeability is significantly increased, typically ranging from 10 to 20 μm^2 . They can be considered as a single-phase medium filled with proppants, allowing for the use of linear flow models to describe the fluid transport behavior in dual-wing fractures.

2.2. Tracer Flowback Principle and Typical Curve. During fracturing construction, the injection–flowback technique using tracer materials is commonly employed to monitor the effectiveness of the fracturing process. As tracers flow through different fracture systems, the resulting tracer injection–flowback curves vary. Analyzing these curves allows for the determination of postfracture fracture morphology and the acquisition of relevant fracture parameters. Moreover, it facilitates the evaluation of different fracturing parameters, guiding reservoir assessment, geological design, fracturing design, and operational procedure development.

The injection–flowback process of tracer materials can be divided into three stages.

- (1) Injection stage: The fracturing fluid containing tracer materials is pumped into the formation and flows into the rock fractures.
- (2) Displacement stage: After the tracer-laden fracturing fluid enters the formation, additional fracturing fluid without tracer materials is pumped to displace the tracer-laden fluid further into the fractures.
- (3) Flowback stage: Periodic sampling and testing of the flowback fluid at the wellhead are conducted to separate and measure the concentrations of different tracer materials, obtaining concentration flowback curves for each tracer.

Tracer materials are initially injected into the formation along with the fracturing fluid, entering the rock fractures. After the fracturing operation is completed and the well is opened, the tracer materials flow back to the wellbore with the returning formation fluids due to the production pressure differential. As a

result, the concentration flowback curve of the dual-wing fracture system typically exhibits an unimodal or multimodal shape, as shown in Figure 1.

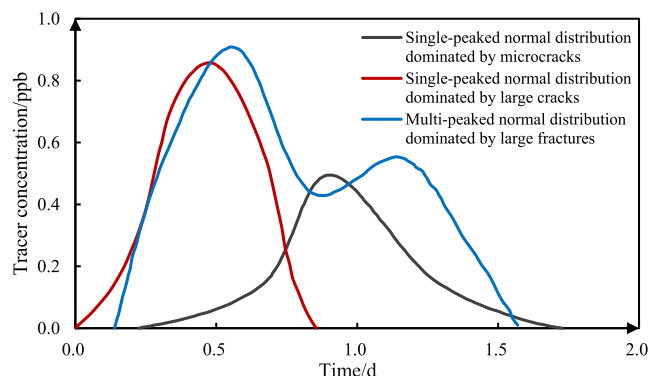


Figure 1. Typical curve of dual-wing fracture tracer flowback.

From Figure 1, we can observe that in fracture systems dominated by microfractures, the flow conductivity is limited. As a result, the concentration of the tracer material changes slowly, exhibiting a gradual increase followed by a slow decline. This pattern approximates an unimodal normal distribution. In fracture systems dominated by large fractures, where the main flow channels for the tracer material are high-conductivity dual-wing fractures, the concentration of the tracer material rises and falls rapidly, resulting in a sharper peak in the concentration curve, resembling an unimodal normal distribution with a more pronounced peak. If multiple dual-wing fractures are involved in the fracturing process and flowback simultaneously, the concentration curve of the tracer material will exhibit a multimodal pattern.

3. MATHEMATICAL MODEL FOR FRACTURING TRACER FLOWBACK

The fractures typically generated by conventional fracturing techniques are generally represented by a single main fracture, as illustrated in Figure 2.

To facilitate the calculation, the simplified physical model is shown in Figure 3.

3.1. Single Dual-Wing Fractures. Based on the characteristics of tracer movement in the fracture with fracturing fluid, the following basic assumptions need to be made:

- (1) The fracturing fluid is continuous and incompressible.
- (2) Tracers, fracturing fluid, and rock do not undergo chemical reactions.
- (3) Although tracers are special agents, they can be treated as water during the injection process for further analysis of tracer movement.
- (4) The influence of gravity and capillary forces on tracer flow is neglected, and the flow of tracers and fracturing fluid is considered as piston-like displacement with a viscosity ratio of 1.
- (5) The flow behavior of fracturing fluid in the fracture follows the Hagen–Poiseuille equation.
- (6) The exchange between the fracture and matrix due to infiltration and absorption is not considered, and the flow of fracturing fluid is assumed to occur only in the fracture.

Taking into account the convective and diffusive effects of tracers, the one-dimensional flow equation for tracers is as follows

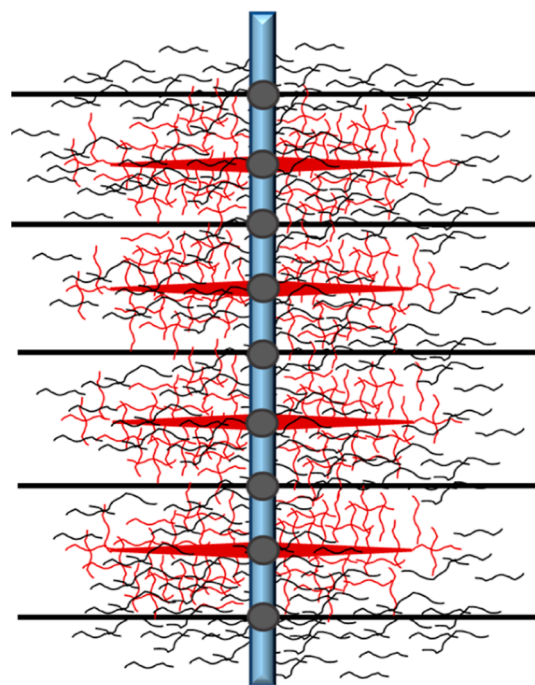


Figure 2. Common fracturing fracture pattern.

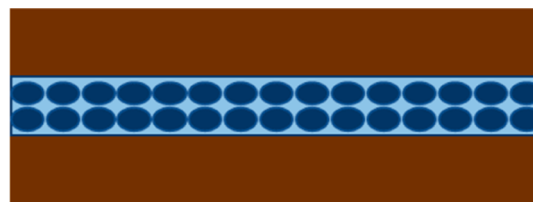


Figure 3. Physical model of double-winged seam tracer flowback.

$$D \frac{\partial^2 C}{\partial x^2} - v_i \frac{\partial C}{\partial x} = \frac{\partial C}{\partial t} \quad (1)$$

The boundary conditions are as follows

$$\begin{cases} C(x, t) = 0 \\ C(\infty, t) = 0 \\ C(0, t) = C_0 \end{cases} \quad (2)$$

where v_i is the tracer flow rate, $\text{m}\cdot\text{s}^{-1}$. C is the tracer concentration, ppb. C_0 is the initial tracer injection concentration, ppb. D is the diffusion coefficient, $\text{m}^2\cdot\text{s}^{-1}$. t is the tracer transport time, s. x is the tracer transport location, m.

After the Laplace transform of eq 1, the solution of the transformed ordinary differential equation can be determined.³⁰ At this point, the ordinary differential equation is as follows

$$D \frac{d^2 \bar{C}}{dx^2} - v_i \frac{d\bar{C}}{dx} - p\bar{C} = 0 \quad (3)$$

where, \bar{C} represents the Laplace transform of C and p is a complex parameter variable.

By performing the transformation, we can convert the original equation into a second-order homogeneous linear equation and solve it to obtain the solution.

$$\bar{C}(x, p) = \frac{C_0}{p} \exp\left(\frac{v_i x}{2D} - x\sqrt{\frac{v_i^2}{4D^2} + \frac{p}{D}}\right) \quad (4)$$

According to the Laplace inverse transform, i.e. $C(x, t) = L^{-1}[\bar{C}(x, p)]$,³¹ the analytical solution of the above equation's fixed solution problem can be obtained as follows

$$C(x, t) = \frac{C_0}{2} \left[\operatorname{erfc}\left(\frac{x - v_i t}{2\sqrt{Dt}}\right) + \exp\left(\frac{v_i x}{D}\right) \operatorname{erfc}\left(\frac{x + v_i t}{2\sqrt{Dt}}\right) \right] \quad (5)$$

where, $\operatorname{erfc}(m)$ is a complementary error function with the expression

$$\operatorname{erfc}(m) = 1 - \operatorname{erf}(m) = \frac{2}{\sqrt{\pi}} \int_x^\infty e^{-\eta^2} d\eta \quad (6)$$

where $\operatorname{erf}(m)$ is the error function.

In a single main fracture, it is known that $\frac{D}{v_i} \ll 0.005$.

Neglecting the second term in the square brackets of eq 5, and considering the infinitesimal tracer segment Δx as a study point, the mathematical model of tracer concentration distribution in a single main fracture can be obtained after differentiation due to the relatively small Δx

$$\frac{C}{C_0} = \frac{\Delta x}{\sqrt{4\pi Dt}} \exp\left[\frac{-(x - v_i t)^2}{4Dt}\right] \quad (7)$$

There is adsorption of the tracer as it percolates through the fracture, so a retention factor R is introduced, and by substituting R into the mathematical equation for one-dimensional percolation of the original tracer, eq 8 is obtained

$$D \frac{\partial^2 C}{\partial x^2} - v_i \frac{\partial C}{\partial x} = R \frac{\partial C}{\partial t} \quad (8)$$

Similarly, considering adsorption and retention effects, the concentration distribution equation for the tracer material after Laplace transformation can be expressed as follows

$$\frac{C}{C_0} = \frac{\Delta x}{\sqrt{4\pi DRt}} \exp\left[\frac{-(Rx - v_i t)^2}{4DRt}\right] \quad (9)$$

From eq 8, it can be inferred that in a fractured reservoir segment with only one main fracture, the dimensionless concentration of the tracer material C/C_0 exhibits a normal distribution with respect to the transport distance, with a symmetric axis along the line $x = \frac{v_i t}{R}$.³²

After injecting fracturing fluid containing tracers into the formation, followed by the injection of tracer-free fracturing fluid, the tracers can be pushed into further fractures. Therefore, using the superposition principle, the mathematical expression for the tracer concentration in the transition phase can be obtained as follows

$$C(x, t) = \frac{C_0 v_i t'}{\sqrt{4\pi DRt}} \exp\left[\frac{-(Rx - v_i t')^2}{4DRt}\right] \quad (10)$$

where, t' is the continuous injection time of the tracer, s .

After the well is shut-in and then reopened for flowback, the movement direction of the tracer is reversed compared to the injection phase. For ease of calculation, let us assume that the tracer injection phase is still ongoing and the tracer is flowing along the fracture. In this case, we can consider the injection and

flowback stages of the tracer in a single well as a "one injection, one production"²² scenario between two wells. Assuming the flowback production point is at $2\frac{v_i t'}{R}$, the mathematical equation for the concentration variation during the flowback stage of the tracer in a single dual-wing fracture is given by eq 11.

$$\begin{aligned} \frac{C}{C_0} &= \frac{v_i t'}{\sqrt{4\pi DR(t_i + t_f)}} \exp\left[-\frac{(R \cdot 2v_i t'/R - v_i t_i - v_f t_f)^2}{4DR(t_i + t_f)}\right] \\ &= \frac{v_i t'}{\sqrt{4\pi DR(t_i + t_f)}} \exp\left[-\frac{(v_i t_i - v_f t_f)^2}{4DR(t_i + t_f)}\right] \end{aligned} \quad (11)$$

where, t_i is the time of the injection phase, s , t_f is the time of the rejection phase, s , v_i is the rate of the injection phase, $m \cdot s^{-1}$, and v_f is the rate of the rejection phase, $m \cdot s^{-1}$.

3.2. Multiple Dual-Wing Fractures. In the fracturing process, there are multiple fractures created. If we assume there are n fractures created, then the expression for the tracer concentration during flowback in the i -th fracture can be given as

$$C_i = \frac{C_0 v_i t'}{\sqrt{4\pi DR(t_i + t_f)}} \exp\left[-\frac{(v_i t_i - v_f t_f)^2}{4DR(t_i + t_f)}\right] \quad (12)$$

The length of the tracer segment is expressed as

$$v_i t' = \frac{V}{nA} = \frac{4V}{n\pi b^2} \quad (13)$$

where, b is the equivalent diameter of the fracture, m . A is the seepage cross-sectional area, m^2 and V is the tracer injection volume, m^3 .

The expressions for the injection and rejection rates are as follows

$$\begin{cases} v_i = \frac{4Q_i}{n\pi b^2} \\ v_f = \frac{4Q_f}{n\pi b^2} \end{cases} \quad (14)$$

where, Q_i is the tracer injection flow rate, $m^3 \cdot s^{-1}$. Q_f is the tracer return flow rate, $m^3 \cdot s^{-1}$.

In mining applications, the effective diffusion coefficient D is commonly calculated using the hydrodynamic diffusion coefficient α . In the absence of molecular diffusion, the diffusion coefficient D can be expressed as a function of hydrodynamic diffusion coefficient α and flow velocity v . The formula is expressed as follows

$$D = \alpha \cdot v \quad (15)$$

where, α is the hydrodynamic diffusivity, m . α represents only the dispersion characteristics of the pore medium and can be derived from experiments.

Substituting eqs 14 and 15 into eq 12 yields

$$\begin{aligned} \frac{C_i}{C_0} &= \frac{V}{\pi \sqrt{R\alpha n b^2 (Q_i t_i + Q_f t_f)}} \\ &\exp\left[-\frac{(Q_i t_i - Q_f t_f)^2}{R\alpha n b^2 \pi (Q_i t_i + Q_f t_f)}\right] \end{aligned} \quad (16)$$

All fractures in the fracture zone are superimposed to yield the final tracer rejection output concentration as follows

$$C_1 = \frac{nq_f C_i}{Q_f} = C_i \quad (17)$$

where, C_1 is the tracer rejection output concentration for multiple fractures, ppb. q_f is the return flow rate for a single fracture, $\text{m}^3 \cdot \text{s}^{-1}$.

Using C_1 instead of C_p , eq 16 is the tracer concentration equation expressed in terms of the fracture equivalent diameter b . Next, the concentration equation expressed in terms of the fracture equivalent permeability is derived.

Assuming that the flow of fracturing fluid in the fracture follows Darcy's law, we can obtain the equation based on Darcy's law and Hagen–Poiseuille law

$$q = \frac{K_f A \Delta p}{\mu l} \quad (18)$$

$$q = \frac{\pi b^4 \Delta p}{128 \mu l} \quad (19)$$

where, q is the flow rate, $\text{m}^3 \cdot \text{s}^{-1}$, K_f is the fracture permeability, μm^2 , μ is the fluid viscosity, $\text{mPa} \cdot \text{s}$, l is the fracture length, m , and Δp is the pressure difference between the two ends of the fracture, MPa .

The relationship between the fracture permeability K_f and the equivalent diameter b of a single fracture can be derived as follows

$$K_f = \frac{b^2}{32} \quad (20)$$

Assuming the average permeability of the fracture zone is K_n , representing the permeability of n parallel fractures, we can obtain the following equation from Darcy's law

$$Q = \frac{K_n n A \Delta p}{\mu l} = nq = n \frac{K_f A \Delta p}{\mu l} \quad (21)$$

We obtain $K_n = K_f$, where, Q is the fracture zone flow rate, $\text{m}^3 \cdot \text{s}^{-1}$.

Based on the average permeability K_n , the mathematical model for the concentration of the tracer material during flowback can be expressed as follows

$$\frac{C_i}{C_0} = \frac{V}{\pi \sqrt{32 R a n K_n (Q_f t_i + Q_f t_f)}} \exp \left[-\frac{(Q_f t_i - Q_f t_f)^2}{32 R a n K_n \pi (Q_f t_i + Q_f t_f)} \right] \quad (22)$$

3.3. Consider Fracture Tortuosity. The actual pressure-opening fractures are not uniformly smooth and are often rough. To describe the fractures more accurately, we need to consider the presence of tortuosity within the fractures. Assuming that the flow of the tracer material in the fracture follows the law of uniform laminar flow and that the fracturing fluid is incompressible, we can establish the motion equation in the X direction as follows

$$\begin{cases} \Delta p h dz + \frac{\partial \tau_x}{\partial z} h l \tau dz = 0 \\ \tau_x = \mu \frac{dv_x}{dz} \end{cases} \quad (23)$$

The derivation leads to

$$v_x = \frac{\Delta p}{2 \mu l \tau} z (s - z) \quad (24)$$

$$Q = \int_0^s v_x h dz = \frac{s^3 h \Delta p}{12 \mu l \tau} \quad (25)$$

where τ is the tortuosity of the fracture, z is the position in the Z direction, m , τ_x is the shear force in the X direction, N , v_x is the flow velocity in the X direction, $\text{m} \cdot \text{s}^{-1}$, h is the fracture height, m , and s is the fracture opening, m .

To simplify the model, we consider the fracture as a rough cylindrical conduit, assuming that fluid flow within the fracture follows the Hagen–Poiseuille equation. Additionally, we assume that during the flow process, the fluid's volume and flow rate remain constant. Therefore, we can derive the following equation

$$Q = \frac{n \pi b^4 \Delta p}{128 \mu l \tau} = \frac{s^3 h \Delta p}{12 \mu l \tau} \quad (26)$$

$$s h l = \frac{1}{4} n \pi b^2 l \quad (27)$$

Next, we can obtain

$$b^2 = \frac{8}{3} s^2 \quad (28)$$

Then the mathematical model of tracer return concentration for fracture opening can be obtained as follows

$$\frac{C_i}{C_0} = \frac{V}{\pi \sqrt{\frac{8}{3} R a n s^2 (Q_f t_i + Q_f t_f)}} \exp \left[-\frac{(Q_f t_i - Q_f t_f)^2}{\frac{8}{3} R a n s^2 \pi (Q_f t_i + Q_f t_f)} \right] \quad (29)$$

In the above mathematical model, the values of parameters such as K_n , n , b , and s for multiple dual-wing fracture seams can be obtained by tracer concentration curve interpretation when parameters such as C_0 , V , Q_f , and Q_f are known.

4. TRACER INJECTION–FLOWBACK CONCENTRATION CURVE INTERPRETATION

During actual field operations, the tracer flowback concentration curves are closely related to the morphology of the fractured formations created during the fracturing. Different postfracturing fracture morphologies result in distinct tracer flowback curves, affecting the curve shape, peak concentration, and tracer arrival time. Therefore, before interpreting tracer flowback curves, it is necessary to understand the differences in fracture characteristics associated with different fracturing techniques. Tracer flowback curves provide a noninvasive method that indirectly reveals the microstructure of the fracture network, which is of significant importance for the development and production of reservoirs.

According to the tracer flowback principles and the physical characteristics of Gaussian function curves, a method called "Gaussian fitting + theoretical equation inversion" has been developed to interpret the concentration curve of tracer flowback. This method allows for the transformation of qualitative assessments of fracture morphology in mining fields into quantitative descriptions and provides insights into key

parameters such as fracture half-length, fracture width, and fracture conductivity.

4.1. Gaussian Fitting Procedure.

- (1) Analyze the on-site tracer flowback monitoring results and plot the concentration curve of tracer flowback.
- (2) Utilize MATLAB programming to perform Gaussian fitting on the monitored tracer concentration curve and assess the fitting performance between the regression equation and the measured data using four parameters: sum of squared errors, coefficient of determination, adjusted coefficient of determination and root-mean-square error.

4.1.1. Sum of Squared Errors (SSE). The sum of squared errors (SSE) between the regression values obtained after fitting and the original data points can be represented by the following equation

$$SSE = \sum_{i=1}^n (y_i - \hat{y}_i)^2 \quad (30)$$

A smaller SSE indicates a better model selection and fitting.

4.1.2. Coefficient of Determination (R-Square). The range of values of the coefficient of determination is [0,1], and the closer the coefficient of determination is to 1, the better the fitting effect.

$$R\text{-square} = \frac{SSR}{SST} = 1 - \frac{SSE}{SST} = \frac{\sum_{i=1}^n (\hat{y}_i - \bar{y})^2}{\sum_{i=1}^n (y_i - \bar{y})^2} \quad (31)$$

4.1.3. Adjusted R-Square. The adjusted coefficient of determination (adjusted R-square) is a modified version of the coefficient of determination (R-square) that takes into account the number of variables in the regression model. It is used to assess the fitting effect by considering the impact of increasing the number of variables. The formula for the adjusted R-square is as follows

$$\text{Adjusted R-square} = 1 - (1 - R^2) \frac{(n - 1)}{(n - k)} \quad (32)$$

A higher value of the adjusted coefficient of determination (adjusted R-square) indicates a better fitting effect.

4.1.4. Root Mean Square Error (RMSE). Root mean square error (RMSE) is a measure of the average squared difference between the predicted values and the actual values of the data. It is calculated by taking the square root of the mean of the squared differences, as shown in the following equation

$$RMSE = \sqrt{\frac{SSE}{n}} = \sqrt{\frac{1}{n} \sum_{i=1}^n (y_i - \hat{y}_i)^2} \quad (33)$$

A smaller RMSE indicates a better model selection and fitting, where, y_i and \hat{y}_i are known values of parameters, mean values, and fitted values, respectively, n is the number of study subjects, and k is the number of variables (generally $k = 2$).

- (3) Based on the number of peaks obtained from fitting the tracer flowback curve, one can estimate the number of fractures and make a rough assessment of the fracture morphology in the formation. A smooth single-peaked curve corresponding to a normal distribution suggests the presence of microfractures. On the other hand, a sharp-peaked curve corresponding to a normal distribution

indicates the existence of highly conductive channels, where the surrounding microfractures can be neglected.

- (4) By analyzing the equation of the fitted tracer flowback curve, one can determine the Gaussian distribution and Gaussian equation corresponding to each peak. This information provides a foundation for subsequent theoretical equation fitting of individual fractures.

4.2. Theoretical Equation Inversion.

- (1) Analyze the Gaussian equations corresponding to the tracer flowback curves for each fracture obtained through Gaussian fitting.

The equation for a Gaussian distribution is as follows:

$$f(x) = \frac{1}{\sqrt{2\pi}\sigma} e^{-(x-\mu)^2/2\sigma^2} + m \quad (34)$$

where $x = \mu$ is the symmetry axis and σ indicates the dispersion of the data. The larger σ is, the more dispersed the data are and the flatter the Gaussian distribution curve. Conversely, the thinner and taller the Gaussian distribution curve is. m is the correction value.

Rewrite the dual-wing fracture tracer return concentration curve eq 9 as

$$C = \frac{\frac{C_0 \Delta x}{R}}{\sqrt{2\pi} \left(\sqrt{\frac{2Dt}{R}} \right)} \exp \left[\frac{-\left(x - \frac{v_i t}{R} \right)^2}{2 \left(\sqrt{\frac{2Dt}{R}} \right)^2} \right] \quad (35)$$

Comparing eqs 34 and 35, we can get $a = \frac{C_0 \Delta x}{R}$, $\sigma = \sqrt{\frac{2Dt}{R}}$, $\mu = \frac{v_i t}{R}$, $m = 0$.

- (2) Substituting the in situ tracer injection rate v_i , tracer transport time t , and tracer injection C_0 concentration into a , σ and μ yields the retention factor, hydrodynamic diffusivity and fracture half-length.

To determine the location of the “assumed return output point”, by comparing eqs 16, 22, and 29 with eq 35, we can obtain the following equation

$$\begin{aligned} & \frac{C_0 V}{\pi \sqrt{R a n b^2 (Q_i t_i + Q_f t_f)}} \\ &= \frac{C_0 V}{\pi \sqrt{32 R a n K_n (Q_i t_i + Q_f t_f)}} \\ &= \frac{C_0 V}{\pi \sqrt{\frac{8}{3} R a n s^2 (Q_i t_i + Q_f t_f)}} \\ &= \frac{1}{\sqrt{2\pi}\sigma} \end{aligned} \quad (36)$$

According to the on-site tracer injection volume V , tracer injection time t_i , tracer return time t_f , tracer injection flow rate Q_i , and tracer return flow rate Q_f , the fracture permeability, fracture conductivity, and fracture opening can be obtained.

5. APPLICATION EXAMPLE

5.1. Interpretation of Fracture Parameters. The experimental data for this example is obtained from a hydraulic fracturing well in a specific block of the Shengli Oilfield in China. We will use the hydraulic fracturing well HD4-3H in the experimental area as an example to interpret the tracer flowback

curve. The well underwent three stages of fracturing, and we will focus on the first stage. The corresponding relationship between a , b , and c can be observed in eq 35. By employing an optimization algorithm, Gaussian fitting was performed, and the equation of the fitted tracer flowback curve is shown in eq 37.

$$f(x) = a_1 \cdot \exp\left(-\left(\frac{x - b_1}{c_1}\right)^2\right) + a_2 \cdot \exp\left(-\left(\frac{x - b_2}{c_2}\right)^2\right) + a_3 \cdot \exp\left(-\left(\frac{x - b_3}{c_3}\right)^2\right) + a_4 \cdot \exp\left(-\left(\frac{x - b_4}{c_4}\right)^2\right) + m \quad (37)$$

The values corresponding to each variable are obtained as shown in Table 1.

Table 1. Values Corresponding to Each Variable

variable	a_1	b_1	c_1
corresponding value	12.93	916.2	39.52
variable	a_2	b_2	c_2
corresponding value	9.512	11.98	9.63
variable	a_3	b_3	c_3
corresponding value	9.65	6.255	775.9
variable	a_4	b_4	c_4
corresponding value	4.15	466.3	865.9

The values of SSE, R-square, adjusted R-square, and RMSE are shown in Table 2.

Table 2. Values Corresponding to the Fitted Characterization Coefficients

fitted characterization coefficients	SSE	R-square	adjusted R-square	RMSE
corresponding value	150.7	0.8136	0.7841	1.961

The fitted Gaussian fit curve for the tracer's factorless concentration is shown in Figure 4.

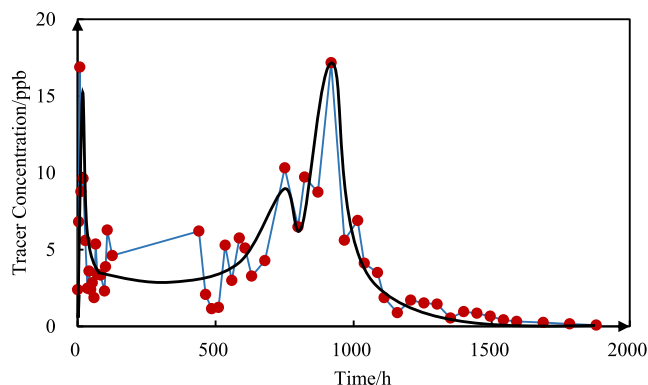


Figure 4. Gaussian fitting curve for tracer factorless concentration.

The width of the tracer flowback curve represents the propagation range of the tracer in the underground reservoir. The height of the curve represents the concentration or arrival time of the tracer. The slope of the curve represents the rate at which the tracer concentration or arrival time changes with distance.

According to Figure 4, it can be observed that the tracer flowback curve in the first time period exhibits a less pronounced single peak, suggesting the presence of microfractures that can be neglected. The characteristics of the second time period are not clear, making it difficult to analyze. In the third and fourth time periods, sharp-peaked curves corresponding to a normal distribution are observed, indicating the presence of two highly conductive fractures with dual-wing morphology.

The fitted curve can be divided into four segments and plotted separately, as shown in Figure 5.

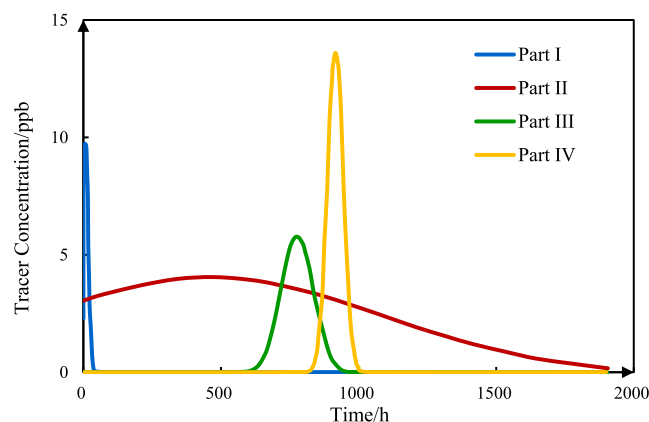


Figure 5. Fitting curves for each component.

By comparing Figures 4 and 5, it can be observed that the third peak primarily corresponds to the first part of the Gaussian fitting equation, while the fourth peak corresponds to the second part of the Gaussian fitting equation. Taking the third peak as an example, the Gaussian fitting equation is as follows

$$f(x) = 12.93 \exp\left(-\left(\frac{x - 916.2}{39.52}\right)^2\right) \quad (38)$$

The comparison shows that $\frac{\Delta x}{\sqrt{4\pi DRt}} = 12.93$, $\mu = \frac{vt}{R} = 916.2$, $2\sigma^2 = \frac{4Dt}{R} = 39.52$. Given that $v_i = 0.6024 \text{ m}\cdot\text{h}^{-1}$, $t = 1761 \text{ h}$, solving for this gives a tracer travel distance of $\Delta x = 79.759 \text{ m}$, tracer retention factor $R = 1.3058$, and combined tracer diffusion coefficient $D = 0.0254$, that is, the fracture half-length $L = 79.759 \text{ m}$. At this point, the "assumed return output point" is at $x = 2\frac{vt}{R} = 1624.8 \text{ m}$. Based on known field construction parameters: tracer volume $V = 1 \text{ m}^3$, injection time $t_i = 1.1351 \text{ h}$, flowback time $t_f = 1762 \text{ h}$, tracer injection flow rate $Q_i = 320.45 \text{ m}^3\cdot\text{h}^{-1}$ and tracer return flow rate $Q_f = 0.41 \text{ m}^3\cdot\text{h}^{-1}$, the calculation yields a fracture diameter $b = 0.00319$, $m = 3.19 \text{ mm}$, which gives a fracture permeability of $267.2 \mu\text{m}^2$, a fracture conductivity of $86.84 \text{ mD}\cdot\text{m}$, and a fracture opening of $s = 0.0037 \text{ m}$. The same was interpreted for the fourth peak and the results are shown in Table 3.

5.2. Results Validation. According to Table 3, the HD4-3H well generated two dual-wing fractures in the target formation during hydraulic fracturing. The field requirement for fracture length is greater than 50 m, and the fracturing effect meets the design values. By comparing the results with the microseismic measurement data at the site, it is found that the fracture lengths obtained from this interpretation method are consistent with the microseismic results.

Table 3. Fracture Parameters

fractures	retention factor	hydrodynamic diffusivity	fracture half-length/m	fracture width/m	fracture opening/m	fracture permeability/ μm^2	fracture conductivity/ $(\mu\text{m}^2\cdot\text{cm})$
fracture 1-1	1.9386	0.0372	24.963	0.00354	0.0051	115.8	43.41
fracture 1-3	1.3058	0.0254	79.759	0.00319	0.0037	267.2	86.84

Using the fracture parameters obtained from the inversion of the flowback curve as input parameters in the numerical model, the accuracy and applicability of the tracer flowback curve interpretation method established in this study are verified through production comparison.

The monitoring of this well lasted for 73 days, with a cumulative production of 792.2 m³ of fluid, 476.9 m³ of oil, and an average water cut of 39.8%. Based on the analysis using oil-soluble tracers, the contribution of the first segment to oil production is 18.65%, equivalent to 90.6 m³ of oil. Based on the analysis using water-soluble tracers, the contribution of the first segment to water production is 15.7%, equivalent to 51.1 m³ of water. The cumulative oil and water production obtained from the CMG simulation are compared with the actual production data, as shown in Table 4.

Table 4. Comparison of Simulated Capacity and Actual Capacity

output	actual value	simulated value	relative error/%
cumulative oil production/m ³	90.6	92.8	2.43
cumulative water production/m ³	51.1	52.9	3.52

By examining Table 4, it can be observed that the relative errors between the calculated results and the actual values are small. This demonstrates that the tracer flowback mathematical model and the interpretation method for the flowback curve established in this study have good applicability in solving practical problems.

6. RESULTS AND DISCUSSION

Based on the establishment of mathematical models and case analysis, this article has derived the following conclusions:

1. Based on the migration characteristics of tracers in fractures during the fracturing process, this article establishes a mathematical model for tracer flowback considering single fractures, homogeneous fracture zones, and the consideration of fracture tortuosity.
2. The article proposes a “Gaussian fitting + theoretical equation inversion” interpretation method for tracer flowback concentration curves. This method can provide output parameters such as fracture half-length, fracture width, and fracture conductivity, enabling the accurate characterization of postfracture fracture features.
3. The comprehensive approach proposed in this article provides more comprehensive and reliable results, demonstrating feasibility for practical applications and enabling rapid implementation in mining sites.
4. By combining field data with production comparisons, the applicability and accuracy of the interpretation method have been verified.
5. Due to the potential complexity of field fracturing conditions, which may result in composite fractures characterized by “high-conductivity fractures + micro-

fractures,” further research is needed to interpret tracer flowback curves for the network of composite fractures.

Overall, the results of this study provide insights into tracer flowback analysis and offer practical implications for reservoir characterization and production optimization. Future research efforts should focus on addressing the challenges posed by composite fractures to further enhance the interpretive capabilities of tracer flowback analysis.

AUTHOR INFORMATION

Corresponding Authors

Dianfa Du – National Key Laboratory of Deep Oil and Gas, School of Petroleum Engineering, China University of Petroleum (East China), Qingdao 266580, China; Email: dudf@upc.edu.cn

Fanghui Hao – National Key Laboratory of Deep Oil and Gas, School of Petroleum Engineering, China University of Petroleum (East China), Qingdao 266580, China; orcid.org/0009-0000-5526-0262; Email: 1710711880@qq.com

Authors

Yuan Li – National Key Laboratory of Deep Oil and Gas, School of Petroleum Engineering, China University of Petroleum (East China), Qingdao 266580, China

Di Li – National Key Laboratory of Deep Oil and Gas, School of Petroleum Engineering, China University of Petroleum (East China), Qingdao 266580, China

Yujie Tang – National Key Laboratory of Deep Oil and Gas, School of Petroleum Engineering, China University of Petroleum (East China), Qingdao 266580, China

Complete contact information is available at:

<https://pubs.acs.org/10.1021/acsomega.3c08411>

Notes

The authors declare no competing financial interest.

ACKNOWLEDGMENTS

This research was supported by the National Key R&D Program of China (Grant no. 2017ZX05072-004). We would like to express our gratitude to Shengli Oilfield for providing the actual data. The authors sincerely thank the editors and reviewers for spending their valuable time reviewing and providing valuable comments.

REFERENCES

- (1) Kathel, P.; Mohanty, K. K. Wettability Alteration in a Tight Oil Reservoir. *Energy Fuels* **2013**, *27* (11), 6460–6468.
- (2) Zhao, X.; Yang, Z.; Zhou, S.; Luo, Y.; Liu, X.; Zhang, Y.; Lin, W.; Xiao, Q.; Niu, Z. Research on Characterization and Heterogeneity of Microscopic Pore Throat Structures in Tight Oil Reservoirs. *ACS Omega* **2021**, *6* (38), 24672–24682.
- (3) Liu, Y.; Dong, X.; Chen, Z.; Hou, Y.; Luo, Q.; Chen, S. Pore-Scale Mobility Evaluation for Tight Oil Enhanced Oil Recovery Methods Based on Miniature Core Test and Digital Core Construction. *Ind. Eng. Chem. Res.* **2021**, *60* (6), 2625–2633.

- (4) Yang, L.; Wang, S.; Jiang, Q.; You, Y.; Gao, J. Effects of Microstructure and Rock Mineralogy on Movable Fluid Saturation in Tight Reservoirs. *Energy Fuels* **2020**, *34* (11), 14515–14526.
- (5) Gai, S.; Nie, Z.; Yi, X.; Zou, Y.; Zhang, Z. Study on the Interference Law of Staged Fracturing Crack Propagation in Horizontal Wells of Tight Reservoirs. *ACS Omega* **2020**, *5* (18), 10327–10338.
- (6) He, P.; Pan, L.; Lu, Z.; Zhou, J.; Meng, C.; Yu, H. Experimental Study to Quantify Fracture Propagation in Hydraulic Fracturing Treatment. *ACS Omega* **2022**, *7* (31), 27490–27502.
- (7) Zolfaghari, A.; Dehghanpour, H.; Ghanbari, E.; Bearinger, D. Fracture Characterization Using Flowback Salt-Concentration Transient. *SPE J.* **2016**, *21* (01), 233–244.
- (8) Clarkson, C. R. R.; Williams-Kovacs, J. D. D. Modeling Two-Phase Flowback of Multifractured Horizontal Wells Completed in Shale. *SPE J.* **2013**, *18* (04), 795–812.
- (9) Zheng, A.; Liu, Q.; Tian, Y.; Fu, Z.; Bai, X. Hydraulic Fracturing Evaluation with Microseismic Monitoring Technique for Shallow Carboniferous Volcanic Rock Reservoirs. *Spec. Oil Gas Reserv.* **2012**, *19* (01), 120–123 + 142.
- (10) Clarkson, C. R.; Yuan, B.; Zhang, Z. A New Straight-Line Analysis Method for Estimating Fracture/Reservoir Properties Using Dynamic Fluid-in-Place Calculations. *SPE Reserv. Eval. Eng.* **2020**, *23* (02), 606–626.
- (11) Kabir, S.; Rasdi, F.; Igboalisi, B. Analyzing Production Data From Tight Oil Wells. *J. Can. Pet. Technol.* **2011**, *50* (05), 48–58.
- (12) Liu, H.; Hu, X.; Guo, Y.; Ma, X.; Wang, F.; Chen, Q. Fracture Characterization Using Flowback Water Transients from Hydraulically Fractured Shale Gas Wells. *ACS Omega* **2019**, *4* (12), 14688–14698.
- (13) Warner, N. R.; Darrah, T. H.; Jackson, R. B.; Millot, R.; Kloppmann, W.; Vengosh, A. New Tracers Identify Hydraulic Fracturing Fluids and Accidental Releases from Oil and Gas Operations. *Environ. Sci. Technol.* **2014**, *48* (21), 12552–12560.
- (14) Grassi, A.; Raudino, A. Modeling Diffusion-Controlled Permeation through a Fractured Surface: Possibility of Estimating the Average Distance among the Fractures by Fluorescence Quenching Measurements. *J. Phys. Chem.* **1996**, *100* (42), 16934–16939.
- (15) Liu, S.; Du, H.; Tian, J.; Zhang, Y.; Liu, J.; Tian, X.; Wang, Z.; Huang, K. Study on an Anti-Adsorption Micromaterial Tracer System and Its Application in Fracturing Horizontal Wells of Coal Reservoirs. *ACS Omega* **2023**, *8* (31), 28821–28833.
- (16) McKay, L. D.; Cherry, J. A.; Bales, R. C.; Yahya, M. T.; Gerba, C. P. A Field Example of Bacteriophage as Tracers of Fracture Flow. *Environ. Sci. Technol.* **1993**, *27* (6), 1075–1079.
- (17) Du, D.; Zhang, Y.; Liu, X.; Zhang, L.; Ren, L.; Liu, P. New Gas Tracer Convection-Diffusion Model between Wells in Heavy Oil Reservoirs. *ACS Omega* **2021**, *6* (38), 24752–24764.
- (18) Jin, C. Technology and Application of Tracer Monitoring and Production Evaluation for Horizontal Well Segmentation Transformation. *Well Test.* **2015**, *24* (04), 38–39 + 42 + 76–77.
- (19) Lichtenberger, G. J. *SPE Production Operations Symposium*; Society of Petroleum Engineers: Oklahoma City, OK, 1991. Field Applications of Interwell Tracers for Reservoir Characterization of Enhanced Oil Recovery Pilot Areas
- (20) Jiang, R.; Jiang, H.; Yang, S. A New Technique for The Analysis of Interwell Tracers. *Acta Pet. Sin.* **1996**, No. 03, 85–91.
- (21) McDaniel, R. R.; Borges, J. F.; Dakshindas, S. S. *All Days*; SPE: Anaheim, California, U.S.A., 2007, p SPE-109969-MS. A New Environmentally Acceptable Technique for Determination of Propped Fracture Height and Width
- (22) Li, L.; Jiang, H.; Li, J.; Zhao, L. *All Days*; SPE: Moscow, Russia, 2016, p SPE-181972-MS. Fracture Quantitative Characterization Using Tracer Flowback for Multistage Fracturing Horizontal Well in Tight Oil
- (23) Duenckel, R. J.; Smith, H. D.; Chapman, M. A.; Saldungaray, P. *All Days*; SPE: Al-Khobar, Saudi Arabia, 2011, p SPE-149102-MS. A New Nuclear Method to Locate Proppant Placement in Induced Fractures
- (24) Wang, L.; Gao, X.; Cui, H. Experimental Study on Radioactive Tracer of Hydraulic Fracturing in Oilfield. *J. Isot.* **2019**, *32* (05), 349–354.
- (25) Guo, H.; Pan, Q.; Zhai, L. The Artificial Fracture Longitudinal Profile Testing Technology in the Application of Hydraulic Fracturing in Daqing Oil Field. *J. Isot.* **2019**, *32* (02), 115–120.
- (26) Tian, W.; Darnley, A.; Mohle, T.; Johns, K.; Dempsey, C. Understanding Frac Fluid Distribution of an Individual Frac Stage from Chemical Tracer Flowback Data. In *Day 2 Wed, February 06, 2019*; SPE: The Woodlands, Texas, USA, ; p D022S005R002.
- (27) Zhong, P.; Lu, F.; You, Y.; Yi, X.; Ao, K. Fitting Method of Fracture Volume Calculation Based on Tracer Monitoring and Its Application. *Drill. Prod. Technol.* **2022**, *45* (04), 109–113.
- (28) Wu, Y.-S.; Pruess, K. Numerical Simulation of Non-Isothermal Multiphase Tracer Transport in Heterogeneous Fractured Porous Media. *Adv. Water Resour.* **2000**, *23* (7), 699–723.
- (29) Datta-Gupta, A.; King, M. J. A Semianalytic Approach to Tracer Flow Modeling in Heterogeneous Permeable Media. *Adv. Water Resour.* **1995**, *18* (1), 9–24.
- (30) Dong, S.; Gong, Y. Application of Laplace Transform in Solution of Improper Integral and Differential Equation. *J. Jiangnan Univ. Sci. Ed.* **2019**, *47* (03), 227–230.
- (31) Teng, Y. Computation of Inverse Laplace Transform. *Stud. Coll. Math.* **2016**, *19* (06), 20–21 + 23.
- (32) Wagner, O. R.; Baker, L. E.; Scott, G. R. *All Days*; SPE: Houston, TX, 1974, p SPE-5125-MS. The Design and Implementation of Multiple Tracer Program for Multifluid, Multiwell Injection Projects.